Biochimica et Biophysica Acta, 978 (1989) 305–312
Elsevier

BBA 74297

Fourier transform infrared spectroscopic studies on the secondary structure of the Ca^{2+}-ATPase of sarcoplasmic reticulum

J. Villalain [1], J.C. Gomez-Fernandez [1], M. Jackson [2] and D. Chapman [2]

[1] *Departamento de Bioquimica, Universidad de Murcia, Murcia (Spain) and* [2] *Department of Protein and Molecular Biology, Royal Free Hospital School of Medicine, London (U.K.)*

(Received 15 July 1988)

Key words: Fourier transform infrared spectroscopy; ATPase, Ca^{2+}-; Sarcoplasmic reticulum; Secondary structure; (Rabbit)

Fourier transform infrared spectroscopy has been applied to the study of the secondary structure of the Ca^{2+}-ATPase of sarcoplasmic reticulum. An attempt is made to quantitatively assess the various secondary structures present. Values of 45% α-helix, 32% β-sheet and 23% turns were obtained. A comparison is made of these results and those obtained using other techniques such as CD and Raman spectroscopy. The various assumptions inherent in the present procedure are discussed. The effect of various ligands, e.g. Ca^{2+}, vanadate, ATP and phosphate, upon the structure were investigated. Upon binding these ligands no marked spectral changes were observed.

Introduction

The Ca^{2+}-transporting ATPase of sarcoplasmic reticulum (EC 3.6.1.38) is one of the best characterized membrane ion transport systems. This enzyme catalyzes the active transport of two moles of Ca^{2+} ions per mole of ATP hydrolyzed (see Ref. 1 for a review on this system).

The primary structure of this protein has been recently deduced from its cDNA sequence and from this data predictions of its secondary structure have been made [2,3]. It has been deduced from electron microscopy studies [4] and from X-ray and neutron diffraction data [5,6] that about 40% of the protein volume lies inside the lipid bilayer whilst the remainder of the protein lies on the outside of the lipid bilayer on the cytoplasmic surface. Combining all of these results [3] the picture which emerges is that the Ca^{2+}-ATPase consists of a major globular part in the cytolasm formed by three domains of β-structure, where these domains are linked between them and to the membrane by α-helical and random elements. The portion of the protein situated inside the membrane is considered to be predominantly α-helical in character.

During the ATP-dependent Ca^{2+} transport cycle, the Ca^{2+}-ATPase undergoes several conformational transitions, characterized by different affinities for Ca^{2+}, ATP and other ligands [1]. During this cycle the calcium-enzyme complex is destabilized by enzyme phosphorylation at the catalytic site [7,1]. These conformational transitions are to be expected for vectorial transport of Ca^{2+}. To attempt to follow such structural changes in the protein it is necessary to use physical techniques that can give information on the spatial organization of this protein. For example, the secondary structure of the Ca^{2+}-ATPase has been probed by spectroscopic techniques, including circular dichroism [8–10] and Raman [11,12] and Fourier transform infrared spectroscopy [13–18]. From the bands in the Amide I region it is possible to detect the presence of α-helical, β-sheet and random coil structures. Application of these and other techniques to the study of the structural implications of ligand binding to the Ca^{2+}-ATPase have however to date resulted in a body of contradictory reports. Thus, no change in protein secondary structure is detected by circular dichroism [9,10]. However a recent FTIR study is reported to show a significant increase in the spectral contribution associated with the α-helical structures [18], whilst laser Raman spectroscopy is reported to show a slight decrease in α-helical conformation [11]. In some of these studies different preparations were used (i.e. some authors have examined sarcoplasmic reticulum membranes [18] whilst others have studied purified Ca^{2+}-ATPase [9]) and this may partly explain the confusion.

Abbreviations: S/N ratio, signal-to-noise ratio; FTIR, Fourier transform infrared spectroscopy; CD, circular dichroism.

Correspondence: D. Chapman, Department of Protein and Molecular Biology, Royal Free Hospital School of Medicine, Rowland Hill Street, London NW3 2PF, U.K.

It is apparent that clarification of the structural basis of Ca^{2+} translocation is required. We have therefore undertaken a study of the possible conformational changes in the secondary structure of the Ca^{2+}-ATPase in the presence and absence of a number of ligands, such as Ca^{2+}, vanadate, ATP and phosphate using FTIR spectroscopy. We use established curve fitting procedures to quantify the secondary structure of the protein. We discuss the problems which arise in the application of such procedures.

Experimental Procedures

Materials

Deuterium oxide (99.8%), ATP and phospho*enol*-pyruvate were obtained from Sigma, UK, and lactate dehydrogenase and pyruvate kinase from Boehringer. All other chemicals used throughout this work were analytical grade also from Sigma.

Preparation of purified Ca^{2+}-ATPase for FTIR measurements

Sarcoplasmic reticulum was prepared from rabbit back and leg white muscles according to the method of Nakamura et al. [19]. Ca^{2+}-ATPase was purified from these membranes by the method of Warren et al. [20] using 0.5 mg of sodium cholate per mg of protein (purified ATPase in H_2O) and procedure 2 of Meissner et al. [21] using 0.2 mg of sodium cholate per mg of protein (purified ATPase in ^2H_2O). Protein was estimated by the method of Lowry et al. [22] as modified by Wang and Smith [23], and Larson et al. [24] using bovine serum albumin as standard or from the ATPase molar absorption [8].

Preparations of purified ATPase were stored before use at $-40\,^{\circ}C$ in 50 mM sucrose, 10 mM Tris-maleate (pH 7.0) at a protein concentration of 25–50 mg/ml. Within four days of purification and before measurements, the preparations were thawed, centrifuged and the pellet resuspended in buffer containing 0.1 M KCl, 10 mM imidazole, 1 mM EGTA, 1 mM $MgCl_2$ (pH 7.4), either in H_2O or in ^2H_2O. This last step was repeated once more, obtaining a final protein concentration of 20 mg/ml. Before FTIR measurements were made, concentrated stock solutions of $CaCl_2$, Na_3VO_4, ATP or Na_2HPO_4, either in H_2O or ^2H_2O buffer were added to the purified Ca^{2+}-ATPase solutions giving final concentrations of 8 μM and 0.1 mM free Ca^{2+}, 5 mM vanadate, 10 μM ATP, 2 mM ATP and 5 mM phosphate. The concentration of free Ca^{2+} was calculated using a computer program that takes into account the concentration of the different molecules in solution [25].

ATPase activity was assayed at $25\,^{\circ}C$ with an ATP regenerating system essentially as described by Gomez-Fernandez et al. [26]. All samples gave an activity between 2 and 3 mmol ATP/mg of protein per min.

FTIR spectroscopy

Infrared spectra of purified ATPase suspensions in ^2H_2O were recorded on a Nicolet MX-1 FT-IR spectrometer assisted by a Nicolet 1200S data station and in H_2O with a Perkin-Elmer 1750 FTIR spectrometer assisted by a Perkin-Elmer 7300 data station. Samples were examined in a Beckman FH-01 CFT thermostated cell equipped with CaF_2 windows separated by a 25 μm Teflon spacer for samples in ^2H_2O and 6 μm tin spacer for samples in H_2O. The spectrometers were continuously purged with dry air to eliminate water vapour absorptions from the spectral region of interest. Either 216 scans for ATPase in ^2H_2O or 200 scans for ATPase in H_2O were recorded at $20\,^{\circ}C$, 2 cm^{-1} resolution and signal averaged. For the ATPase in H_2O a sample shuttle was used to record spectra ratioed against the background over the scanning period. Buffer spectra, either in H_2O or in ^2H_2O, were recorded under the same temperature and scanning conditions as the corresponding protein spectra. Each sample was equilibrated at the chosen temperature and conditions for at least 10 min before data aquisition. Subtracted spectra were digitized (0.9645 cm^{-1} and 1 cm^{-1} data point increment for the Nicolet and Perkin-Elmer spectrometers, respectively) and transferred to an Olivetti M-24 computer were all data analysis was made. Overlapping infrared bands were resolved by Fourier deconvolution and Fourier derivation [27] and band-fitting analysis was performed using established procedures [28,29].

Results

Infrared spectra of Ca^{2+}-ATPase in H_2O and ^2H_2O media

The most useful band in the infrared spectra of proteins for structural analysis is the Amide I band. This band, however, usually has a very broad band contour. This is because it consists of several overlapping components which are assigned to specific secondary structures, such as α-helix, β-sheet, turns, non-ordered segments. Bands corresponding to amino acid side chains also appear. The Amide I and Amide II regions of the infrared spectra of purified ATPase in H_2O and ^2H_2O buffer are shown in Figs. 1A and 1D, respectively. Due to the hydrogen-deuterium exchange of the amide groups, the maximum of the Amide I band shifts from 1655 cm^{-1} in H_2O to 1648 cm^{-1} in ^2H_2O and the Amide II band shifts from 1547 cm^{-1} in H_2O to 1460 cm^{-1} in ^2H_2O. The region from 1600 to 1520 cm^{-1} in ^2H_2O contains residual bands due to slowly exchanging amide hydrogens.

Due to the large intrinsic widths of the individual components present they cannot be resolved by increasing instrumental resolution. For this it is necessary to

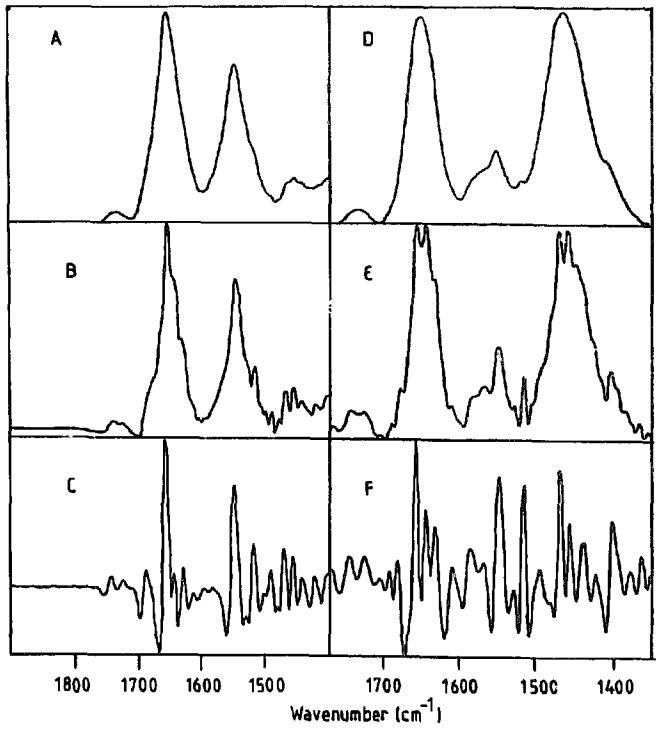

Fig. 1. Amide I and Amide II regions of the infrared spectra of the purified Ca^{2+}-ATPase from sarcoplasmic reticulum in H_2O buffer (A, B and C) and ^2H_2O buffer (D, E and F). (A, D) Original spectra, (B, E) Fourier deconvolved spectra (90% Lorentzian bandshape, resolution enhancement factor of 2.1 and bandwidth of 15 cm^{-1}), and (C, F) Fourier derivative spectra (power of 3 and breakpoint of 0.25). See text for more details. Redrawn from originals.

rely upon application of several qualitative and quantitative methods which recently have been developed. The qualitative computational methods which have been recently introduced for band narrowing are Fourier deconvolution and Fourier derivation (Refs. 27, 30 and references therein). These methods, given the correct input parameters and working on spectra of good resolution and signal-to-noise ratio (S/N ratio), provide the number and frequencies of the component bands which form the original band contour.

Fourier deconvolution is an iterative procedure controlled by three adjustable parameters, i.e., band-width, resolution enhancement factor and bandshape (Lorentzian, Gaussian or mixed), whereas Fourier derivation is controlled by one adjustable parameter, the breakpoint, which controls the resolution enhancement. The limits of the resolution enhancement factor are determined by the S/N ratio, resolution of the spectrometer and the lineshape (the resolution enhancement factor is always higher for Lorentzian bandshapes than for Gaussian bandshapes).

In order to choose the best parameters for Fourier deconvolution and Fourier derivation we monitored the S/N ratio of the 1900–1800 cm^{-1} region of the spectrum which is free of any absorption (see for example Fig. 1A). For Fourier deconvolution we have used 90% Lorentzian/10% Gaussian[30] bandwidth of 15 cm^{-1} and a resolution enhancement factor of 2.1, which gives a final S/N ratio of 150 and minimal negative lobes (see Figs. 1B and 1E), whereas four Fourier derivation we have used a power of 3 [27] and a breakpoint of 0.25, which corresponds to a smoothed fourth derivative, giving a final S/N ratio of 110 (Figs. 1C and 1F). Much care has to be taken in the use of these procedures. It is not possible to rely on peak heights of the enhanced spectra as a measure of the relative proportion of protein secondary structure as bandshapes can be severely distorted depending on the parameters used for the band-narrowing process as well as upon the bandwidths of the component bands.

Figs. 1 and 2 show the result of Fourier derivation and deconvolution carried out on the spectra of the Ca^{2+}-ATPase in H_2O and ^2H_2O. The component bands of the Amide I band can be attributed, in accordance with the classical correlations in the literature, to the different types of secondary structures present. The major components in the Amide I region of the purified Ca^{2+}-ATPase appear at 1657 and 1646 cm^{-1}. The band at 1656 cm^{-1} in H_2O can be assigned to α-helical segments of protein. The band at 1646 cm^{-1} has previously been assigned to random structures [31]. However, no shift is seen in the frequency of this band upon deuteration. We therefore suggest that this band may be attributed to α-helices as suggested by Lee et al. [15]. Two other bands which appear at 1667 and 1634 cm^{-1}, have been assigned to turns and β-sheet secondary structure, respectively. All assingments made in this work are taken from Refs. 31–33. The simultaneous appearance of two bands, a relatively strong band at 1630 cm^{-1} and a weaker band at 1675 cm^{-1}, are often assigned to antiparallel β-sheet structures. Recent studies [34] however suggest that it is not possible to distinguish between parallel and antiparallel β-sheets. We have therefore assigned the bands which appear at 1679 and 1634 cm^{-1} to β-sheet structures without further definition. The remaining bands are weak ones which have been assigned to turns (band at 1689 cm^{-1}), β-structure (band at 1623 cm^{-1}) and amino acid side chains (band at 1613 cm^{-1}). The band appearing at 1657 cm^{-1} has been assigned to α-helix. However, the reduction in the frequency of the Amide I maximum upon deuteration suggests that random structures are also absorbing in this region in H_2O.

Search for ligand-induced conformational changes in the Ca^{2+}-ATPase

In order to detect conformational changes in the Ca^{2+}-ATPase, spectra were taken first in the presence of 1 mM EGTA. It is assumed that as no free Ca^{2+} is left in this case, the protein will be present in the so called E_1 conformation [35]. Other additions were 8 μM and 0.1 mM free Ca^{2+}, so that the high affinity sites of

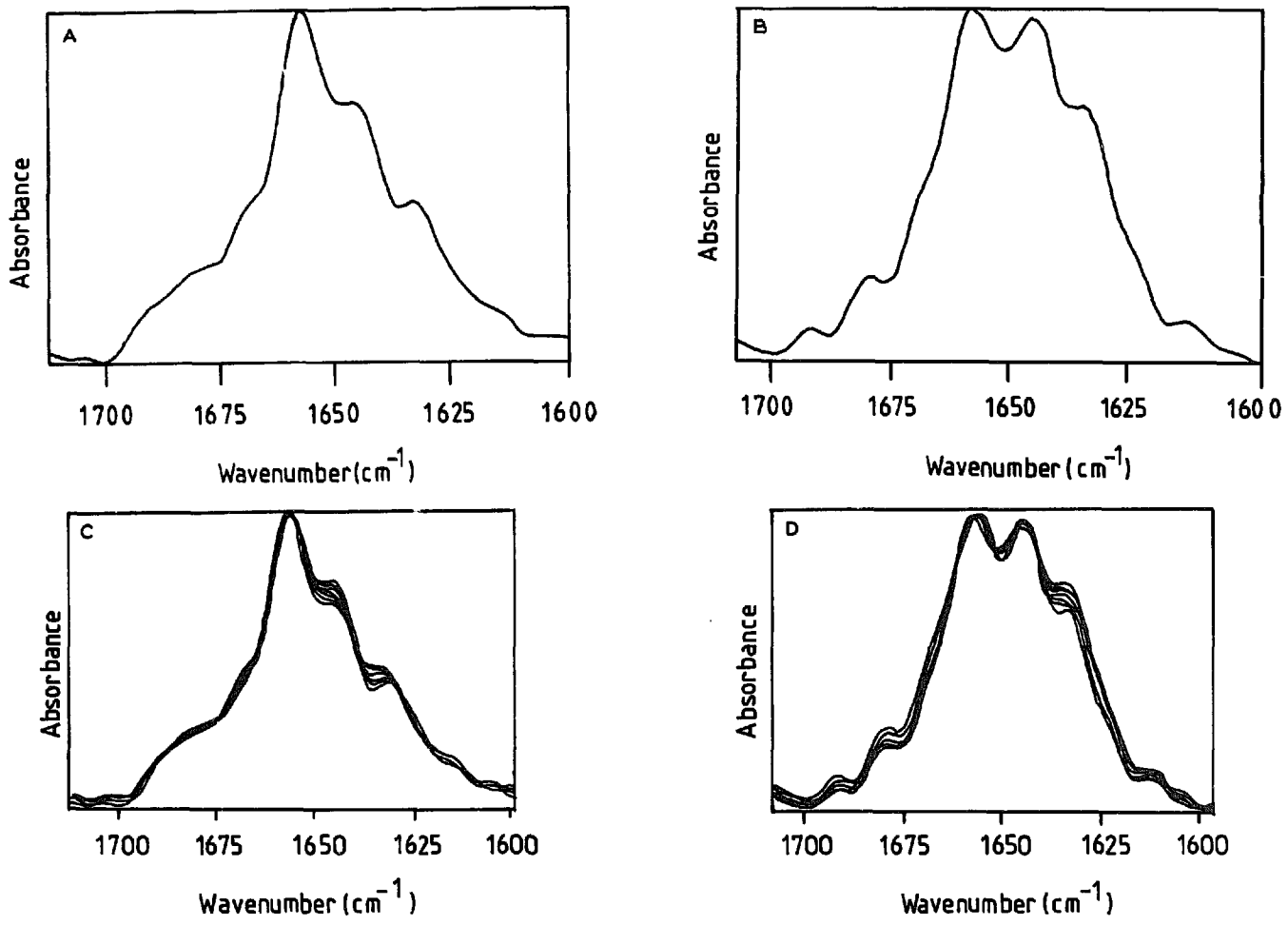

Fig. 2. Fourier deconvolved spectra (90% lorentzian band shape, resolution enhancement factor of 2.1 and bandwidth of 15 cm^{-1}) of the purified Ca^{2+}-ATPase in (A) H_2O buffer containing 1 mM EGTA (B) ^2H_2O buffer containing 1 mM EGTA (C) deconvolved spectra of the Ca^{2+}-ATPase in each of the reaction mixtures (in H_2O) superimposed (D) deconvolved spectra of the Ca^{2+}-ATPase in each of the reaction mixtures (in ^2H_2O) superimposed (see text for more details). Redrawn from originals.

Ca^{2+} will be then occupied and the enzyme will be in the E_1-Ca conformation [35]. Vanadate and inorganic phosphate, which in a calcium-free medium stabilize the E_2 conformation, giving the E_2-P and E_2-V forms, respectively [36,37], were also studied. The addition of ATP was also studied at low (10 μM) and high (2 mM) concentrations. It has been proposed that ATP may bind to the enzyme with different affinities in the absence of free Ca^{2+}: low (μM) and high (mM) affinities [38]. The addition of ATP is therefore to ascertain whether the binding of ATP to the enzyme at different concentrations induces any detectable conformational change.

Fig. 2C shows the superimposed deconvolved spectrum of the Amide I region of samples of the Ca^{2+}-ATPase in H_2O buffer to which the various ligands were added. It is evident that only very minor changes in frequency and intensity occur. Similar results were obtained when the experiments were performed in ^2H_2O media (Fig. 2D). Comparisons were also made using Fourier derivation of the spectra, both in ^2H_2O and H_2O, (spectra not shown). No significant changes were detected in the presence of the various ligands.

Quantification of the secondary structure of the Ca^{2+}-ATPase

It is well known that infrared bands are close to Lorentzian [30] at least for simple molecules, so in order to obtain meaningful results either by Fourier deconvolution or band-fitting analysis Lorentzian bandshapes or bandshapes with a small percentage of Gaussian contribution are generally used. Throughout this work Fourier deconvolution with 90% Lorentzian bandshapes has been applied, The results of such an analysis is illustrated in Fig. 2A. The best band-fitting analysis which can be made with the information obtained from the deconvolution shown in Fig. 2A can be seen in Fig. 3A. Ideally the band-shapes used for the band-fitting analysis should be the same as those used for the Fourier deconvolution. It can be seen however from Fig. 3A that the band-fitting obtained is very poor (partly due to the fact that Lorentzian bandshapes have

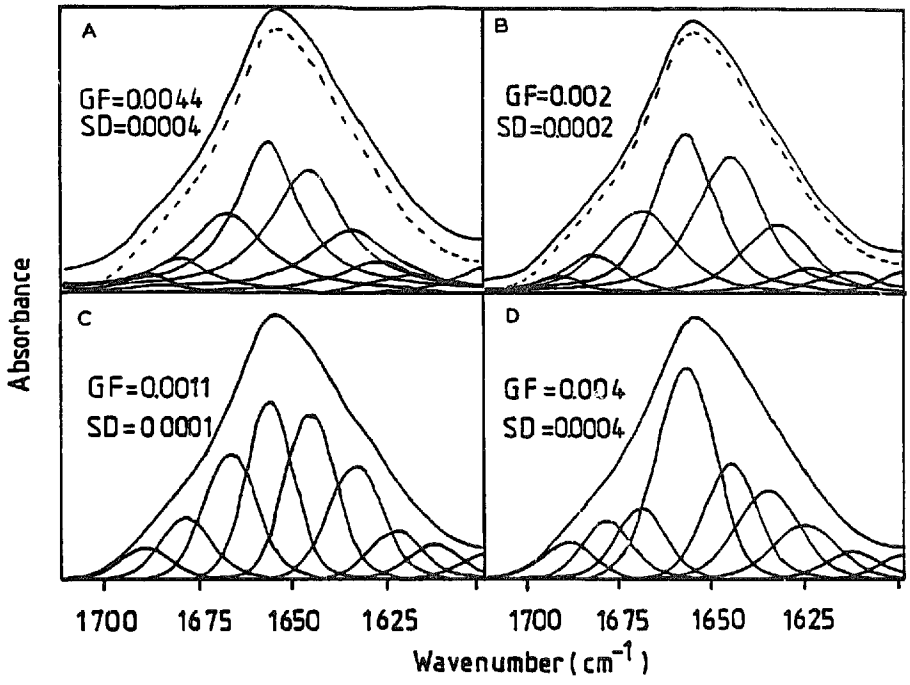

Fig. 3. Band-fitting of the purified Ca^{2+}-ATPase in the presence of 1 mM EGTA, assuming (A) 90% Lorentzian bandshape (B) 50% Lorentzian/50% Gaussian bandshapes (C) 100% Gaussian band shape (D) 100% Gaussian bandshape, with the band at 1657 cm^{-1} arranged to be 32% in area. Solid lines are synthetic curves generated from the individual bands, broken lines are the original spectra (indistinguishable in C and D). Redrawn from originals. GF, goodness of fit; SD, standard deviation of the fit.

large wings). Increasing the Gaussian contribution to the band shapes greatly improves the band-fitting results. This is clearly seen in Fig. 3B, assuming the bands have 50% Gaussian character. In fact the best results are obtained if the bands are assumed to be 100% Gaussian (Fig. 3C). It can be seen from Fig. 3C that a very good curve fit has been obtained, with minimal differences between the experimental and the synthetic spectra. The use of 100% Gaussian shaped bands for band-fitting is a procedure used by a number of authors to fit the 100% Lorentzian deconvolution of the original spectrum [31,33,34]. Some authors do not mention the bandshape used for making the band-fitting analysis of the original spectrum [39–42].

It should be stressed that a good fit cannot be judged by visual inspection. Fig. 3D shows the result of a band fitting in which the area under one of the component curves (centered at 1657 cm^{-1}) was arranged to increase from 23% to 32%. Visually, the fit appears as good as that obtained in Fig. 3C. However, calculation of the goodness of fit (chi^2) reveals that the fit is actually much worse, and is in fact similar to that obtained assuming 10% Gausian bands.

The component bands derived from the band fitting analysis are shown in Fig. 3C. Referring to this figure, eight components can be seen and the percentage of each one over the total area (excluding the amino acid side chain band) are shown in Table I. In order to assess the relative contribution of each type of secondary structure present it is assumed that all of the component bands have the same molar absorption coefficient.

Similar band-fittings were also made for the purified Ca^{2+}-ATPase in the presence of the various ligands, with the protein in H_2O and in ^2H_2O (only the E_1 conformation), always beginning with the deconvolved spectrum as shown in Fig. 2. In all the cases the best band-fitting was always obtained using 100% Gaussian bandshapes and the same number of bands were identified in each experiment. In all cases the frequencies of the various components did not change by more than 0.5 cm^{-1}. Some band frequency changes were observed in the presence of ATP but no significant changes in area occurred. The meaning of this changes in frequency is not clear. Nevertheless, if the addition of ATP causes a conformational change in the protein, it is not a major one.

TABLE I

Band-fitting analysis of purified Ca^{2+}-ATPase in 1 mM EGTA

H_2O media		^2H_2O media		Assignment
frequency (cm^{-1})	%	frequency (cm^{-1})	%	
1689.5	4.1	1692.5	0.7	turns
1678.9	8.8	1679.4	7.4	β-sheet
1667.3	18.6	1666.8	14.9	turns
1656.7	23.1	1656.3	25.6	α-helices
1645.7	22.3	1645.1	23.8	α-helices
1633.8	16.3	1634.2	19.7	β-sheet
1623.4	6.8	1623.7	7.9	β-turns

The area contributed to the band envelope by each individual component in the presence of each ligand does not change by more than 1%. These results indicate that there are no appreciable changes in the protein secondary structure upon ligand binding.

Discussion

Quantitative estimation of the secondary structure of the Ca^{2+}-ATPase

During the past two years a number of studies have been reported which analyse quantitatively the secondary structure of various proteins using FTIR spectroscopy [31,33,34,39–44]. The procedures used are based on band-narrowing techniques such as Fourier deconvolution and Fourier derivation techniques which identify the number and position of component bands. This information is then used as the input parameters for band-fitting analysis of the original or, in some cases, the deconvolved spectrum. The integrated intensities obtained for the different fitted bands are then related to the relative population of the conformational structures represented by these bands (α-helix, β-sheet, etc.). For water soluble proteins agreement with X-ray crystallography data has been good with predictions agreeing to within 4% (see Ref. 31 for a brief review). We will compare results obtained using this method for our membrane protein with results obtained using other techniques.

The secondary structures present in the Ca^{2+}-ATPase has been estimated using different approaches (see Table II). On the basis of the aminoacid sequence, it has been predicted that the Ca^{2+}-ATPase consist of an intramembranous, primarily helical domain, and several cytoplasmic domains composed of α-helical, β-sheet, β-turn and random elements [2,3]. In accordance with these predictions, the α-helix content will amount to 52%, β-sheet, 12%, and β-turns and random elements, 36%. Circular dichroism studies of sarcoplasmic reticulum vesicles give the following composition: 46% α-helix, 8% β-sheet, 13% β-turn and 33% random coil [10]. Raman spectroscopic studies made with light sarcoplasmic reticulum and reconstituted ATPase also agreed with the predominantly α-helical structure of the protein: 50% α-helix, 21% β-sheet, 17% β-turns and 12% random elements [12]. It should be noted that Williams et al. use a completely different way of band-fitting to that normally used for vibrational infrared spectroscopy and their Raman spectra had a very poor S/N ratio.

TABLE II

Quantitative estimation of secondary structure

	CD [a]	AA [b]	Raman [c]	FTIR [d]
α-Helix	46%	52%	50%	45%
β-Sheet	8%	12%	21%	32%
turns	13%		17%	23%
Random	33%		11%	

[a] From Ref. 10.
[b] From Ref. 3, amino acid analysis (AA).
[c] From Ref. 12.
[d] Present communication.

Our results (Table II), show the percentage of α-helical structures of the purified Ca^{2+}-ATPase, assuming 100% Gaussian shaped bands. There is some ambiguity in the assignment of the bands. If we assign the band at 1646 cm^{-1} to random structures the α-helical content would be only 23% of the secondary structure. This is much lower than the other estimations.

Furthermore, when we deliberately arrange the band fitting so as to increase the relative importance of the band centered at 1657 cm^{-1} (assigned to α-helix), so as to increase the α-helix content the resultant curve fitting becomes inadequate. See for example Fig. 3D, where the band at 1656 cm^{-1} accounts for 32% of the total area. If we assign the band at 1646 cm^{-1} also to α-helical structures the α-helical content becomes 45%. In deconvolved and fourth derivative spectra of the protein in ^2H_2O we see no shift in this band, which suggests that the more common assignment of this band to random structures is incorrect. We assign this band to α-helices as previously suggested [15]. The amount of β-sheet predicted from our study amounts to 32% of the secondary structure. This is more than has been calculated by other procedures (see Table II). Finally, β-turns, account for 23% of the secondary structure.

The application of FTIR spectroscopy to the quantitative analysis of the secondary structure of membrane proteins must be approached with caution. The technique used at the present time requires a number of assumptions. These are (a) the band assignments are based primarily upon studies of water soluble proteins, (b) application of curve fitting and deconvolution require assumption of a band shape, e.g. Gaussian, Lorentzian or mixed, (c) it is assumed that all component bands have the same shape and (d) the assumption that all protein secondary structures have equal molar absortivities.

Other techniques of course have their limitations. Circular dichroism, for example, is known to be seriously limited for the study of membrane proteins due to light scattering effects. Raman spectroscopy is limited as the spectra obtained normally have poor S/N ratio, which makes accurate resolution of individual components within the Amide I band envelope impossible. The method used for the band-fitting analysis of Raman data is also somewhat limited. The band-fitting analysis which is currently used fits the spectrum by comparison with the composite data of a number of water-soluble proteins. Application of this technique to membrane proteins assumes that the main band frequencies are the same for water-soluble and membrane

proteins. The FTIR and Raman spectra of bacteriorhodopsin, however, show that at least for this protein the main α-helical band is anomalously high compared to that which is observed for the water-soluble proteins. The general application of water-soluble protein data to membrane proteins is therefore unreliable. Finally, predictions made on the bases of amino acid sequence can be taken only as rough approximations.

Retention of secondary structure between enzymatic states of the Ca^{2+}-ATPase

From our results obtained with purified Ca^{2+}-ATPase, it is apparent that the transitions involved in the enzyme mechanism are not accompanied by major reorganizations of the protein secondary structure. We have considered seven different enzyme states by manipulations of the reaction mixture. The ligand-free enzyme which is obtained here in the presence of 1 mM EGTA, is taken as the reference state. This form is proposed to undergo a structural rearrangement upon cooperative binding of calcium to high-affinity transport sites [45]. This rearrangement has been observed using techniques such as tryptophan fluorescence [46] and electron spin resonance (ESR) spectroscopy [47]. Another transition in the enzyme structure is proposed upon formation of the phosphoenzyme by addition of P_i deduced from low-angle X-ray diffraction [6] or TNP-ATP fluorescence [48]. Vanadate will produce an enzyme-vanadate complex, similar to the phosphoenzyme, with formation of two-dimensional crystals [49]. The binding of ATP at different concentrations to the enzyme depleted of calcium may also produce a conformational change upon binding to the nucleotide binding site, as seen by tryptophan fluorescence [50].

Our studies show that it is not possible, using FTIR spectroscopy, to detect any major change in the secondary structure of the purified ATPase in the presence of various ligands (see Fig. 2). This conclusion agrees with results obtained from circular dichroism using sarcoplasmic reticulum preparations applied to Ca^{2+} binding or formation of vanadate complex [10]. They also agree with circular dichroism experiments performed on the purified Ca^{2+}-ATPase, with respect to calcium-binding and phosphoenzyme formation [9]. Our results differ from previous conclusions obtained by FTIR spectroscoy [18]. However, Arrondo et al. studied sarcoplasmic reticulum vesicles where other proteins present may also contribute to the IR spectrum, and we have studied the purified Ca^{2+}-ATPase. Our band fitting analysis shows that it is possible to measure frequency changes in the presence of ATP (but not in the presence of calcium, vanadate or phosphate) in those bands which we assign to β-structure and aminoacid side chains.

It has been predicted from the amino acid sequence [3] that the nucleotide binding, phosphorylation and transduction domains of the Ca^{2+}-ATPase are composed of predominantly β-sheet secondary structure and are separated from the calcium binding domain (α-helix). Since the calcium and phosphorylation sites of the enzyme are located in different regions of the enzyme and separated by about 40 Å [51], a coordinated conformational change of the Ca^{2+}-ATPase must take place during the catalytic cycle, in order to facilitate the reciprocal influence of calcium binding and phosphorylation [1]. If significant secondary structure changes are not taking place in these domains during this process (as shown here) it must be assumed that twisting and reorientation of polypeptide segments are responsible for the protein conformational changes which accompany the catalytic cycle.

Acknowledgements

This work was supported by CAICYT (Spain), grant No. 0822/84 (to J.C.G.-F.) NATO grant No. 8610712 (to J.C.G.-F. and D.C.) and the Wellcome Trust (M.J.) We also thank Dr. Hector L. Casal for providing the computer programs used in this work as well as his many useful suggestions.

References

1 Inesi, G. (1985) Annu. Rev. Physiol. 47, 573–601.
2 MacLennan, D.H., Brandl, C.J., Korczak, B. and Green, N.M. (1985) Nature 316, 696–700.
3 Brandl, C.J., Green, N.M., Korczak, B. and MacLennan, D.H. (1986) Cell 44, 597–607.
4 Taylor, K.A., Dux, L. and Martonosi, A. (1986) J. Mol. Biol. 187, 417–427.
5 Herbette, L., Defoor, P., Fleischer, S., Pascolini, D., Scarpa, A. and Blasie, J.K. (1985) Biochim. Biophys. Acta 817, 103–122.
6 Blasie, J.K., Herbette, L., Pascolini, D., Skita, V., Pierce, D. and Scarpa, A. (1985) Biophys. J. 48, 9–18.
7 Jenks, W. (1980) Adv. Enzymol. 51, 75–106.
8 Hardwicke, P.M.D. and Green, N.M. (1974) Eur. J. Biochem. 42, 183–193.
9 Nakamoto, R.K. and Inesi, G. (1986) FEBS Lett. 194, 258–262.
10 Csermely, P., Katopis, C., Wallace, B.A. and Martonosi, A. (1987) Biochem. J. 241, 663–669.
11 Lippert, J.L., Lindsay, R.M. and Schultz, R. (1981) J. Biol. Chem. 256, 12411–12416.
12 Williams, R.W., McIntyre, J.D., Gaber, B.P. and Fleischer, S. (1986) J. Biol. Chem. 261, 14520–14524.
13 Cortijo, M., Alonso, A., Gomez-Fernandez, J.C. and Chapman, D. (1982) J. Mol. Biol. 157, 597–618.
14 Mendelsohn, R., Anderle, G., Jaworsky, M., Mantsch, H.H. and Dluhy, R.A. (1984) Biochim. Biophys. Acta 775, 215–224.
15 Lee, D.C., Hayward, J.A., Restall, C.J. and Chapman, D. (1985) Biochemistry 24, 4364–4373.
16 Arrondo, J.L.R., Urbaneja, M.A., Goni, F.M., Macarulla, J.M. and Sarzala, G. (1985) Biochem. Biophys. Res. Commun. 128, 1159–1163.
17 Jaworsky, M. (1985) Biochemistry 24, 3422–3428.
18 Arrondo, J.L.R., Mantsch, H.H., Mullner, N., Pikula, S. and Martonosi, A. (1987) J. Biol. Chem. 262, 9037–9043.

19 Nakamura, H., Jilka, R.L., Boland, R. and Martonosi, A. (1976) J. Biol. Chem. 251, 5414–5423.
20 Warren, G.B., Toon, P.A., Birdstall, N.J.M., Lee, A.G. and Metcalfe, J.C. (1974) Proc. Natl. Acad. Sci. USA 71, 622–626.
21 Meissner, G., Cooner, G. and Fleischer, S. (1973) Biochim. Biophys. Acta 298, 246–269.
22 Lowry, O.H., Rosebrough, N.J., Farr, A.L. and Randall, R.J. (1951) J. Biol. Chem. 193, 265–275.
23 Wang, C.-S. and Smith, R.L. (1975) Anal. Biochem. 63, 414–417.
24 Larson, E., Howlett, B. and Jagendorf, A. (1986) Anal. Biochem. 155, 243–248.
25 Fabiato, A. and Fabiato, F. (1979) J. Physiol. (Paris) 75, 463–505.
26 Gomez-Fernandez, J.C., Goni, F.M., Bach, D., Restall, C.J. and Chapman, D. (1980) Biochim. Biophys. Acta 598, 502–516.
27 Moffatt, D.J., Kauppinen, J.C., Cameron, D.G., Mantsch, H.H. and Jones, R.N. (1986) Computer Programs for Infrared Spectrophotometry, N.R.C.C. Bulletin No. 18, Ottawa, Canada.
28 Fraser, R.D.B. and Suzuki, E. (1966) Anal. Chem. 38, 1770–1773.
29 Fraser, R.D.B. and Suzuki, E. (1969) Anal. Chem. 41, 37–39.
30 Cameron, D.G. and Moffatt, D.J. (1984) J. Testing Evaluation 12, 78–85.
31 Susi, H. and Byler, D.M. (1986) Methods Enzymol. 130, 290–311.
32 Chirgadze, Y.N., Fedorov, O.V. and Trushina, N.P. (1975) Biopolymers 14, 679–694.
33 Byler, D.M. and Susi, H. (1986) Biopolymers 25, 469–487.
34 Susi, H. and Byler, D.M. (1987) Arch. Biochem. Biophys. 258, 465–469.
35 De Meis, L. and Vianna, V. (1979) Annu. Rev. Biochem. 48, 275–292.
36 Masuda, H. and de Meis, L. (1973) Biochemistry 12, 4581–4585.
37 Pick, U. and Karlish, J.D. (1982) J. Biol. Chem. 257, 6120–6126.
38 Dupont, Y. (1977) Eur. J. Biochem. 72, 185–190.
39 Surewicz, W.K., Moscarello, M.A. and Mantsch, H.H. (1987) Biochemistry 26, 3881–3886.
40 Surewicz, W.K., Mantsch, H.H., Stahl, G.L. and Epand, R.M. (1987) Proc. Natl. Acad. Sci. USA 84, 7028–7030.
41 Surewicz, W.K., Moscarello, M.A. and Mantsch, H.H. (1987) J. Biol. Chem. 262, 8598–8602.
42 Surewicz, W.K., Szabo, A.G. and Mantsch, H.H. (1987) Eur. J. Biochem. 167, 519–523.
43 Yang, P.W., Mantsch, H.H., Arrondo, J.L.R., Saint-Girons, I., Guillon, Y., Cohen, G.N. and Barzu, O. (1987) Biochemistry 26, 2706–2711.
44 Surewicz, W.K., Stepanik, T.M., Szabo, A.G. and Mantsch, H.H. (1988) J. Biol. Chem. 263, 786–790.
45 Inesi, G., Kurzmack, M., Coan, C. and Lewis, D. (1980) J. Biol. Chem. 255, 3025–3031.
46 Dupont, Y. (1976) Biochem. Biophys. Res. Commun. 71, 544–550.
47 Coan, C. and Inesi, G. (1977) J. Biol. Chem. 252, 3044–3049.
48 Watanabe, T. and Inesi, G. (1982) J. Biol. Chem. 257, 11510–11516.
49 Dux, L. and Martonosi, A. (1983) J. Biol. Chem. 258, 11903–11907.
50 Dupont, Y., Bennett, N. and Lacapere, J.J. (1982) Ann. N.Y. Acad. Sci. USA 402, 569–572.
51 Scott, T.C. (1985) J. Biol. Chem. 260, 14421–14423.